A POLARIZING BEAM SPLITTING COATING FABRICATED WITH THE USE OF THE WAVELENGTH-INDIRECT BROADBAND OPTICAL MONITORING METHOD[1**]

Q. Lv [1,2], S. Deng [1], Ch. Li [3], M. Huangm [2], G. Li [1*], Y. Jin [1]

[1] Key Laboratory of Chemical Lasers, Dalian Institute of Chemical Physics, Chinese Academy of Sciences, Dalian 116023, China; e-mail: lig@dicp.ac.cn
[2] School of Materials Science & Engineering, Dalian University of Technology, Dalian 116024, China
[3] Bureau of Major R&D Programs, Chinese Academy of Sciences, Beijing 100864, China

We present a testing method based on the use of wavelength-indirect broadband optical monitoring. A polarizing beam splitting (PBS) coating applied at a wavelength of 1550 nm at an incidence angle of 45° was designed. The optimized coating structure contained 59 non-quarter-wave (QW) layers. Preproduction error analysis was used to estimate the advantages of the application of wavelength-indirect broadband optical monitoring. Then, we deposited the PBS coating with an optimized monitoring strategy by ion beam sputtering (IBS). Finally, reverse engineering of the produced PBS coatings was executed. The experimental results show that a good agreement between the theoretical target and the measured transmittance is obtained, the maximum error in the first and last two layers is about 10%, and the minimum error is only about 0.01%.

Keywords: *ion beam sputtering, wavelength-indirect broadband optical monitoring, polarizing beam splitting.*

ПОЛЯРИЗУЮЩЕЕ ПОКРЫТИЕ, ИЗГОТОВЛЕННОЕ С ИСПОЛЬЗОВАНИЕМ МЕТОДА ШИРОКОПОЛОСНОГО СПЕКТРАЛЬНОГО МОНИТОРИНГА

Q. Lv [1,2], S. Deng [1], Ch. Li [3], M. Huangm [2], G. Li [1*], Y. Jin [1]

УДК 535.51

[1] Даляньский институт химической физики Китайской АН, Далянь 116023, Китай; e-mail: lig@dicp.ac.cn
[2] Даляньский технологический университет, Далянь 116024, Китай
[3] Бюро научно-исследовательских программ Китайской АН, Пекин 100864, Китай

(Поступила 7 марта 2018)

Представлен метод контроля толщины покрытия, основанный на использовании широкополосного спектрального мониторинга. Разработано поляризующее покрытие, функционирующее на λ = 1550 нм при угле падения света 45°. Оптимизированная структура покрытия содержит 59 слоев, не являющихся четвертьволновыми. На стадии подготовки образца с целью оценки преимуществ метода широкополосного спектрального мониторинга выполнен анализ погрешностей. Поляризующее покрытие нанесено методом ионно-лучевого напыления с использованием оптимизированного метода мониторинга. Осуществлен реверс-инжиниринг изготовленного покрытия. Получено хорошее соответствие измеренного пропускания с теоретически предсказанным, причем максимальное отклонение между ними в первых и последних двух слоях ~10%, а минимальное ~0.01%.

Ключевые слова: *ионно-лучевое распыление, широкополосный спектральный мониторинг, поляризующее покрытие.*

** Full text is published in JAS V. 86, No. 6 (https://www.springer.com/journal/10812) and in electronic version of ZhPS V. 86, No. 6 (http://www.elibrary.ru/title_about.asp?id=7318; sales@elibrary.ru).

Introduction. The successful fabrication of optical coatings with complex spectrum requirements [1, 2], such as notch filters, multi-bandpass filters, and polarizing beam splitters [3–5], can be technologically demanding. The main problem lies in accurately controlling the layer thickness. Owing to this, optical controlling techniques having a high accuracy of thickness control are extensively applied for multilayer deposition [6–8]. Optical monitoring can be divided into the single wavelength (SWLOM) and broadband (BBOM) methods [9, 10]. Single wavelength optical monitoring cannot be used for controlling the ultra-thin coating due to its intrinsic defects. Thus, the development of nanotechnologies needs an effective broadband optical monitoring technique [11–14].

BBOM is characterized by erroneous self-compensation, higher precision, and adaptation to non-quarter-wave film deposition [15]. However, the lack of a detector and the corresponding spectrometer in a wide spectral range from UV to IR has always been a problem [16].

In this paper, a BBOM system with a monitoring wavelength range from 450 to 1000 nm was employed to control the layer thickness. This means that an optical coating can be monitored only in the range from 450 to 1000 nm when being deposited. It is known that for optical coatings whose working wavelength is out of this range (450–1000 nm), it is impossible to control the layer thickness using direct wavelength monitoring. We propose to control such optical coatings by BBOM, which is an indirect wavelength monitoring method differing from indirect position monitoring mentioned in other reports [9, 17].

In this paper, a PBS coating applied at a wavelength of 1550 nm at an incident angle of 45º was designed and deposited by dual ion beam sputtering (DIBS) [3, 18–21]. The optimized structure contained 59 non-quarter-wave layers. Preproduction error analysis was used to estimate the advantages of the application of wavelength-indirect broadband optical monitoring. Using the wavelength-indirect broadband optical monitoring strategy, the PBS coating deposition was successfully monitored. The advantage of this method for wavelength-indirect monitoring was demonstrated by reverse engineering.

Experimental. *Equipments.* The PBS was fabricated by dual ion beam sputtering (DIBS). Ta_2O_5 and SiO_2 were used as high and low refractive index coating materials, respectively. The physical deposition rate of Ta_2O_5 was ~0.40 nm/s, and that of SiO_2 was ~0.60 nm/s. The coating machine was equipped with a 425 mm diameter planetary fixture and a BBOM system using intermittent transmission monitoring through the center of one of the planets. Figure 1 shows the scheme of the BBOM system [15]. As can be seen in Fig. 1, a broadband light from the source travels through a fiber. The beam is reflected by a mirror and transmits through the substrate from the backside. Then the beam is reflected by another mirror, travels through another fiber, and is finally collected by the spectrometer [22]. The monitoring wavelength range is shown in Fig. 2a. Various materials can be used as the monitoring witness substrate. In this paper, fused silica was chosen as the substrate. The diameter of the sample substrates is 25.4 mm.

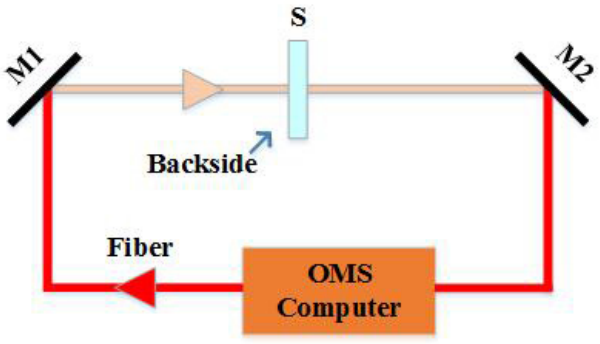

Fig. 1. Scheme of the BBOM system. M1 and M2 are the reflection mirrors; S is the witness substrate; OMS is the optical monitoring system operating computer.

Design. Optilayer was employed to design a PBS coating applied at a wavelength of 1550 nm and an angle of incidence of 45°. The refractive indexes of Ta_2O_5 and SiO_2 were obtained by fitting the transmission spectrum by a well-known matrix method. The refractive indexes n of Ta_2O_5 and SiO_2 were described by the well-known Cauchy formula:

$$n(\lambda) = A_0 + A_1/\lambda^2 + A_2/\lambda^4, \quad (1)$$

where A_0, A_1, and A_2 are the Cauchy dispersion coefficients and λ is the wavelength.

The transmittance of *p*-polarized light for the coating with the optimized design was more than 99.99% (without considering the reflection of the backside) at a 45º angle of incidence. The initial design was based on a standard quarter-wave stack, which contained 59 layers and provided enough optimizable variables to realize high transmittance (99.99%). The theoretical transmission spectrum without the backside reflection and the stack structure of the final optimized design coating are shown in Fig. 2. From Fig. 2c, it can be seen that there are no thin layers. It should be easy to control the thicknesses of these layers accurately by BBOM. However, the working wavelength of this film stack is out of the range of the monitoring wavelength as mentioned above. The layer thickness cannot be monitored using wavelength-direct monitoring when the monitoring wavelength is out of the working wavelength range. Thus, wavelength-indirect BBOM is proposed and employed to monitor the layer thickness of the PBS in this paper.

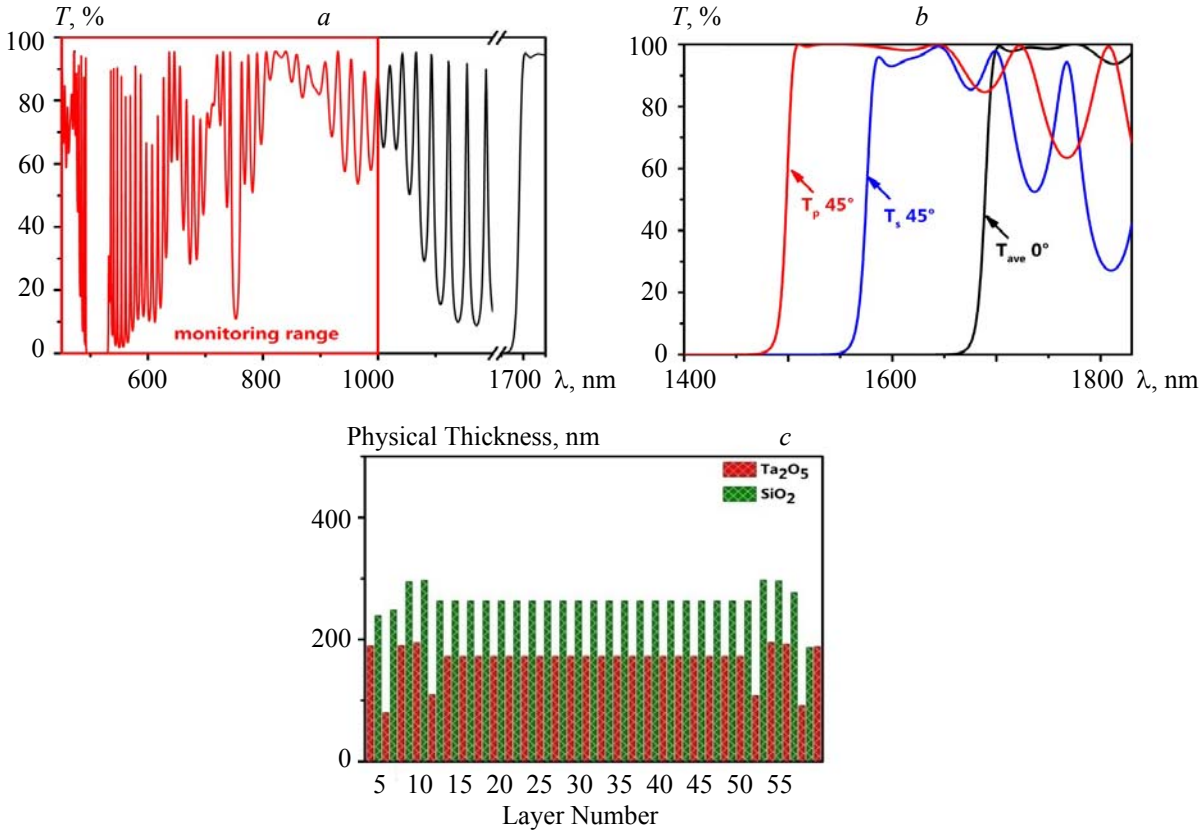

Fig. 2. The theoretical design results of the PBS coating; (a) the theoretical transmittance of the PBS coating, the wavelength ranging from 450–1750 nm; (b) the theoretical transmittance of the PBS coating, the wavelength ranging from 1400–1830 nm; the red curve represents the *p* polarized transmittance at a 45° angle of incidence; the blue curve represents the s polarized transmittance at a 45° angle of incidence; the black curve represents the average transmittance at a normal incidence; (c) the design thickness of the PBS coating.

Broadband optical monitoring method. The BBOM system is employed to control the layer thickness. The BBOM system can obtain the real-time coating related parameters (e.g., deposition rate and refractive index) by fitting the real time measured transmission spectrum with the help of the well-known matrix method to calculate a stop-time prediction that most closely matches the target thickness for this layer. It contains a variety of algorithms for controlling quarter-wave and non-quarter-wave coatings, using in-situ measurements of the transmission spectrum of the monitoring witness. In general, the merit function (F) of the BBOM can be described as

$$F = \sum_{\lambda}[T_{\text{meas}}(\lambda) - T_{\text{targ}}(\lambda)], \quad (2)$$

where $T_{\text{meas}}(\lambda)$ is the measured transmittance and $T_{\text{targ}}(\lambda)$ is the target transmittance.

When BBOM is used, the transmission spectrum of each layers *in situ* measured by the broadband optical monitoring system is fitted and the real-time refractive index and deposition rate can be obtained. Then the stop time is calculated based on the chosen thickness. The deposition time is determined by the equation [15]

$$t_{\text{stop}} = h_{\text{film}}/n_{\text{fit}}v_{\text{fit}}, \tag{3}$$

where t_{stop} is the deposition time, h_{film} is the optical thickness of each layer, n_{fit} is the fitted refractive index, and v_{fit} is the fitted deposition rate.

Results and discussion. To estimate the potential advantage of wavelength-indirect monitoring, a preproduction error analysis for different monitoring wavelength ranges is executed. According to [23], the following equations provide the algorithm for estimating the impact of random errors on the production errors in the case when BBOM is used

$$\alpha_j^i = -\sum_{\{\lambda_k\}}\left(\frac{\partial T^j}{\partial d_j}\frac{\partial T^j}{\partial d_i}\right)\Bigg/\sum_{\{\lambda_k\}}\left(\frac{\partial T^j}{\partial d_j}\right)^2, \tag{4}$$

$$\sigma(\beta_i) = -\sigma_{\text{meas}}/\sum_{\{\lambda k\}}(\partial T^j/\partial d_j)^{1/2}, \tag{5}$$

$$\mu_j^i = \sum_{k=1}^{j-1}\alpha_j^k\mu_k^i \quad \text{for } i = 1, ..., j-1,\ \mu_j{}^i = 1, \tag{6}$$

$$\sigma_j = \left[\sum_{i=1}^{j}(\mu_j^i)^2\sigma^2(\beta_i)\right]^{1/2}, \tag{7}$$

where T is the transmittance, d is the layer thickness; $\{\lambda_k\}$ is the wavelength grid; and σ_{meas} is the standard deviation.

For the preproduction estimation of errors in the layer thickness, Optilayer is employed to simulate the random errors. As mentioned above, only the wavelength range from 450 to 1000 nm can be employed to monitor the layer thickness during the deposition process in this paper. Thus, wavelength-indirect BBOM is employed to monitor the layer thickness instead of wavelength-direct BBOM, whose working wavelength range is covered by the monitoring wavelength range. In addition, considering the refractive index dispersion of the witness substrate in the range from 450 to 600 nm, the wavelength range from 600 to 1000 nm is also discussed. Preproduction estimation of errors in the layer thickness was performed under the assumption that σ_{meas} was 0.2% [23]. It was assumed that BBOM preproduction estimations of errors were performed at 501 evenly distributed wavelengths points in the spectral regions 450–1000, 600–1000, and 1400–1830 nm. The thickness errors are calculated using the 0.2% level of random errors in the transmittance data [23]. Figure 3 shows the expected levels of errors in the thickness of layers of the PBS coating. As can be seen, for both three monitoring strategies, the influence of random errors on the accuracy of the thickness monitoring is quite small. However, the wavelength-indirect monitoring method generates fewer errors. Combined with the discussion above, the wavelength range from 600 to 1000 nm is chosen as the monitoring wavelength range.

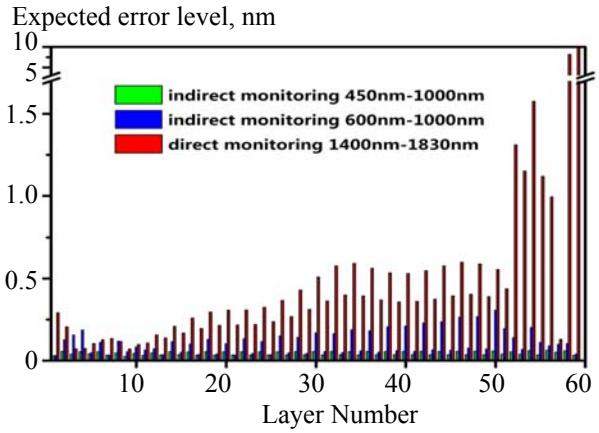

Fig. 3. The expected levels of errors in the thickness of layers of the PBS coating. The green columns represent indirect monitoring in the range 450–1000 nm; the blue columns represent indirect monitoring in the range 600–1000 nm; the red columns represent direct monitoring in the range from 1400 to 1830 nm.

Figure 4 shows the *in situ* monitoring results of the comparison between the theoretical transmittance and the real time measured transmittance of the PBS coating, which is obtained just after the deposition. As can be seen, the theoretical transmittance, real time measured transmittance and real time fitting transmittance agree well. The real time measured transmittance indicates that the PBS coating is successfully and critically deposited by the monitoring wavelength range from 600 to 1000 nm. However, the monitoring range from 600 to 1000 nm is out of the working range from 1400 to 1830 nm. Thus, the capability of the wavelength-indirect BBOM monitoring of the PBS coating requires further discussion.

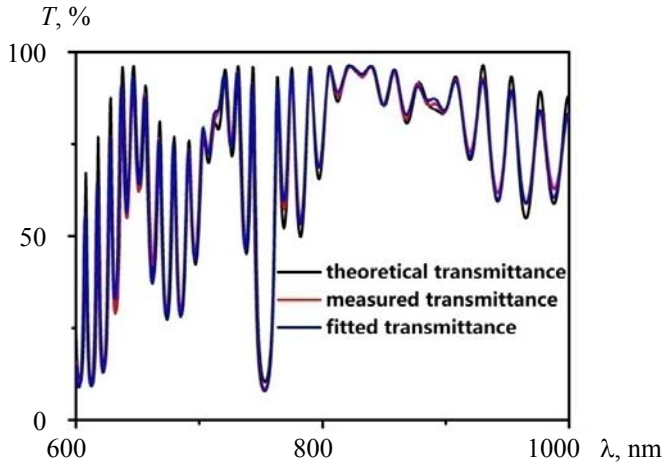

Fig. 4. The theoretical target, the *in situ* measured and fitted transmittance of the PBS coating in the range from 600 to 1000 nm; the black curve represents the theoretical target profile; the red curve represents the in situ measured profile; the blue curve represents the fitted profile.

Broadband light from the source travels through the substrate vertically. This means that the layer monitoring can be performed only for the normal incidence. However, the coating designed in this paper can only be used at a 45º incident angle. On the basis of this, for further study, a spectrophotometer is employed to measure the *ex situ* transmittance of the PBS coating. Figure 5 shows the real measured transmittance of the PBS coating at a 45º angle of incidence in the range from 1400 to 1830 nm. Both the *p*- and *s*-polarized PBS coatings exhibit good performance.

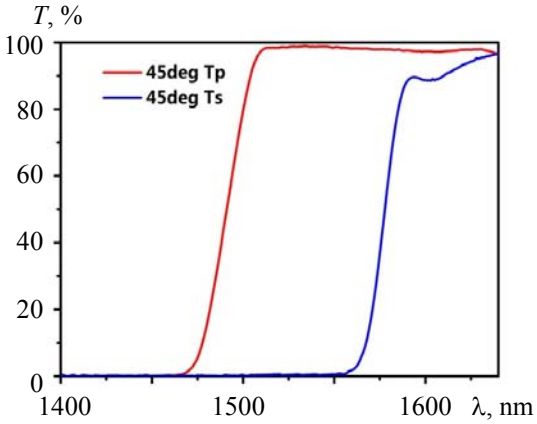

Fig. 5. The measured transmittance p polarized light (red line) and s polarized light (blue line) of the PBS coating (AOI = 45º) in the range from 1400 to 1830 nm

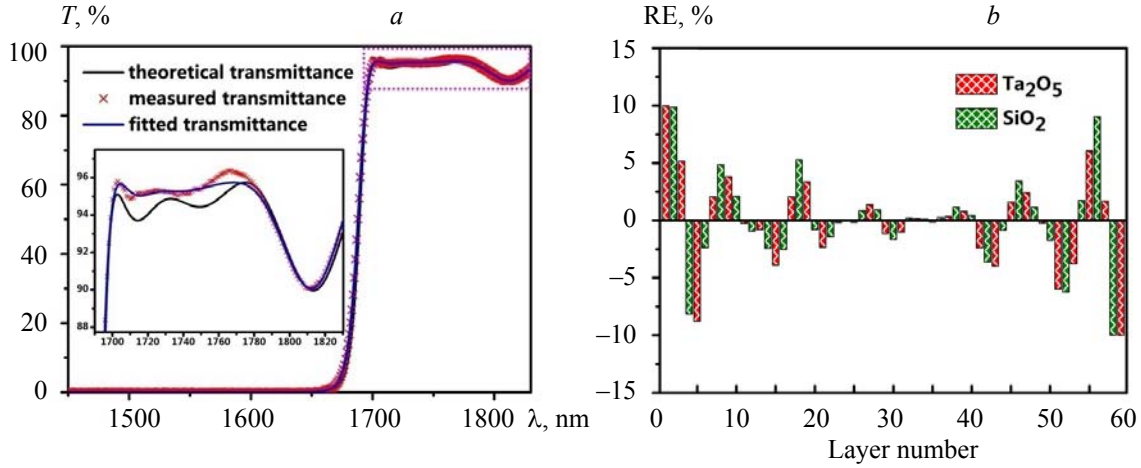

Fig. 6. The measured transmittance (solid curve) and the fitting model transmittance (red crosses) when the model with random errors in the thicknesses of all layers was applied (a) and the relative thickness errors of the PBS coating determined by the reverse engineering procedure (b).

As mentioned above, the IBS method was employed to fabricate the PBS coatings because of its stable deposition rate, which can significantly reduce the defects of the coating, such as the refractive index inhomogeneity. We fulfilled reverse engineering of the produced PBS coatings using OptiRE software to clarify the relative errors in each layer [23]. Figure 6a displays the measured transmittance of the PBS coating at a normal incidence and the fitting model transmittance when the model with random errors in the thicknesses of all layers was used. Relative errors in all layers were obtained and shown in Fig. 6b. It can be seen that the errors vary. It seems that the error in the first and last two layers is about 10% and much larger than those in the other layers due to less signal obtained at the beginning and end of the deposition process. The minimum error is about –0.01%, and the negativity means that the real thickness of the third layer is thinner than expected.

Conclusion. A polarizing beam splitting coating applied at a wavelength of 1550 nm at a 45° angle of incidence was designed by Optilayer and deposited by DIBS. Wavelength-indirect broadband optical monitoring was employed to monitor the layer thickness during the deposition process. The results showed that a polarizing beam splitter can be successfully fabricated by IBS using wavelength-indirect BBOM. Finally, good agreement between the theoretical target and the measured transmittance was obtained; the maximum error in the first layer was about 10%, and the minimum error in the third layer was only about –0.01% based on the results of the reverse engineering analysis.

REFERENCES

1. B. Vidal, E. Pelletier. *Appl. Opt.*, **18**, No. 22, 3857–3862 (1979).
2. B. Vidal, A. Fornier, E. Pelletier. *Appl. Opt.*, **17**, No. 7, 1038–1047 (1978).
3. M. Lappschies, B. Görtz, D. Ristau. *Appl. Opt.*, **45**, No. 7, 1502–1506 (2006).
4. J. Zhang, M. Fang, Y. Jin, H. He. *Chin. Phys. B*, **21**, No. 1, 199–203 (2012).
5. W. Kong, Z. Shen, S. Wang, J. Shao, Z. Fan, C. Lu. *Chin. Phys. B*, **19**, No. 4, 304–308 (2010).
6. H. A. Macleod. Appl. Opt., **20**, No. 1, 82–89 (1981).
7. O. Lyngnes, U. Brauneck, J. Wang, R. Erz, S. Kohli, B. Rubin, J. Kraus, D. Deakins. *Proc. SPIE*, **962715**, 962715–962718 (2015).
8. C. J. Laan. *Appl. Opt.*, **25**, No. 5, 753–760 (1986).
9. J. Zhang, C. Cao, A. V. Tikhonravov, M. K. Trubetskov, A. Gorokh, X. Cheng, Z. Wang. *Appl. Opt.*, **54**, No. 11, 3433–3439 (2015).
10. F. Lai, X. Wu, B. Zhuang, Q. Yan, Z. Huang. *Opt. Express*, **16**, No. 13, 9436–9442 (2008).
11. B. Badoil, F. Lemarchand, M. Cathelinaud, M. Lequime. *Appl. Opt.*, **46**, No. 20, 4294–4303 (2007).
12. A. V. Tikhonravov, M. K. Trubetskov, T. V. Amotchkina. *Appl. Opt.*, **50**, No. 9, C111-C116 (2011).
13. L. Li, Y. Yen. *Appl. Opt.*, **28**, No. 14, 2889–2894 (1989).

14. B. Vidal, A. Fornier, E. Pelletier. *Appl. Opt.*, **18**, No. 22, 3851–3856 (1979).
15. Q. P. Lv, S. W. Deng, S. Q. Zhang, F. Q. Gong, G. Li. *Chin. Phys. B*, **26**, No. 5, 057801 (2017).
16. H. Tao, Y. Wu, J. Chen, Y. Kong, Y. Chen, B. Sun, C. Xu, P. Zhou, J. Qiu, Y. Zheng. *Rev. Sci. Instrum*., **76**, No. 8, 083118–083114 (2005).
17. V. G. Zhupanov, E. V. Klyuev, S. V. Alekseev, I. V. Kozlov, M. K. Trubetskov, M. A. Kokarev, A. V. Tikhonravov. *Appl. Opt.*, **48**, No. 12, 2315–2320 (2009).
18. G. X. Liang, P. Fan, J. G. Hu, J. Zhao, X. H. Zhang, Z. K. Luo, H. L. Ma, J. T. Luo, Z. H. Zheng, D. P. Zhang. *Solar Energy*, **136**, 650–658 (2016).
19. G. X. Liang, P. Fan, X. M. Cai, D. P. Zhang, and Z. H. Zheng. *J. Electron. Mater.*, **40**, No. 3, 267–273 (2011).
20. I. W. Martin, R. Nawrodt, K. Craig, C. Schwarz, R. Bassiri, G. Harry, J. Hough, S. Penn, S. Reid, R. Robie, S. Rowan. *Classical Quant. Grav.*, **31**, No. 3, 035019 (2014).
21. J. T. Brown. *Appl. Opt.*, **43**, No. 23, 4506–4511 (2004).
22. Q. Cai, Y. Zheng, D. Zhang, W. Lu, R. Zhang, W. Lin, H. Zhao, L. Chen. *Opt. Express*, **19**, No. 14, 12969–12977 (2011).
23. A. V. Tikhonravov, M. K. Trubetskov, T. V. Amotchkina. *Appl. Opt.*, **45**, No. 27, 7026–7034 (2006).